Kovove Mater. 62 2024 389–405
DOI: 10.31577/km.2024.6.389

Vanadium in copper-graphite composite

Selim Burak Cantürk[1,2]*, Andrej Opálek[2], Tomáš Dvorák[2], Lukáš Karafa[2], Juraj Koráb[2], Miroslav Čavojský[2], Ľubomír Orovčík[2], Zuzana Hájovská[2], Jaroslav Longauer[2], Naďa Beronská[2], Jaroslav Kováčik[2]

[1] *Faculty of Mechanical Engineering, Slovak University of Technology, Námestie slobody 17, 812 31 Bratislava, Slovak Republic*
[2] *Institute of Materials and Machine Mechanics, Slovak Academy of Sciences, Dúbravská cesta 9, 845 13 Bratislava, Slovak Republic*

Received 17 September 2024, received in revised form 25 November 2024, accepted 27 November 2024

Abstract

The effect of vanadium on the physical properties of Cu-graphite composite was investigated for the first time. There is only one other mention up to now in the scientific literature: Cu-V-Gr composites were prepared by the stir casting process. Their mechanical properties, coefficient of friction, and wear were investigated. In this work, a Cu-graphite composite with 36.3 vol.% of copper was prepared by gas pressure infiltration of the coarse grain graphite powder mixture with and without 1 vol.% of vanadium powder with molten copper. The microstructure of composites was investigated via SEM, TEM, and HRTEM. XRD analysis indicated and HRTEM observation confirmed that V_8C_7 carbide was present at the Cu-graphite interface and in the copper matrix. The copper-graphite interface has a sharp transition between the copper and V_8C_7 phases. The diffusion layer at the borders with graphite is around 75 nm thick. The created vanadium carbide improved the mechanical but worsened thermophysical properties of the prepared Cu-graphite composites. Therefore, vanadium addition is not attractive for Cu-graphite composite industrial applications that require good thermophysical properties.

Key words: vanadium, vanadium carbides, copper, graphite, gas pressure infiltration, mechanical properties, physical properties

1. Introduction

Copper-graphite composites are widely used in various industrial applications such as heat sinks, thermal management, electric brushes, sliding contacts, and seals [1]. The added elements or compounds that affect Cu-graphite interface properties are used in various applications. These elements are often various carbide-forming elements – Si, Ti, Zr, Cr, B, W, Mo, Ni, Fe, etc. All these elements aim to improve the strength between the copper matrix and graphite phase by creating an interface between copper and carbon. Moreover, adding different elements results in using these composites in different applications. In the case of gas pressure infiltration, these elements also affect the wettability of graphite with copper, which is necessary for sound infiltration.

Hongbao Wang et al. observed for Cu-Cr (1.0 wt.%) alloy on graphite substrate reduction of contact angle down to 43° at 1300 ℃ during sessile drop experiments [2]. Wenfu Wei used W to coat the graphite preform to reduce the wetting angle from 138.5° to 23° at the electrical conductivity of the composite (15.1×10^5 S m^{-1}) [3]. The wear rate and corrosion resistance of Cu/5 wt.% SiC-graphite reinforcement are very low and very high, respectively. This composite is anticipated to have practical applications in heat exchangers and other thermal management applications [4]. Ren Zhang et al. investigated Cu/C-1.0 wt.% Zr composite as a suitable candidate for thermal management applications [5]. Thermal conductivity 640 W m^{-1} K^{-1} at the X-Y plane was measured. Haozi Zuo et al. solved the wettability problem of copper-carbon composite by adding Fe [6].

*Corresponding author: e-mail address: selim.canturk@savba.sk

The addition of Fe dropped the wetting angle from 124° to 21°, and C/Cu-3 wt.% Fe composites exhibited a flexural strength of 124.4 MPa and a compressive strength of 378.5 MPa, and the electrical resistivity was 1.8 μΩ m.

Titanium is one of the most used carbide-forming elements employed for different applications, and TiC significantly improves hardness and wear resistance. Carlos R. Rambo infiltrated Ti-Cu alloy into carbon preform: composites are interesting for electrical-mechanical applications as electric discharge machining (EDM) electrodes due to their low electrical resistivity (15–60 μΩ cm) [7]. Peng Xiao et al. investigated the tribological properties of Cu-Ti/C composite prepared via infiltration [8]. Recently, boron became a carbide-forming element that reduced the wetting angle. Haozi Zuo et al. improved the wettability between copper and carbon from 123.6° to 21.3° at 2.5 wt.% B addition [9]. Cu/C-1.2 wt.% B composite produced via infiltration showed low electrical resistance (1.7 μΩ m), and the authors claimed that this composite could be a promising candidate for electrical contact materials.

Vanadium is another carbide-forming element. Vanadium has never been used to create an interface between copper and graphite so far in copper-graphite composites. Jabinth et al. [10] work deals with vanadium and graphite reinforcement in copper matrix. They prepared pure Cu, Cu-2V, Cu-2V-0.5Gr, Cu--2V-1Gr, and Cu-2V-1.5Gr by stir casting. The XRD analysis did not confirm significant copper, graphite, and vanadium reactions. The increase in vanadium and graphite content led to decreased copper grain size. This led to enhanced strength, impact strength, and hardness, to decreased the coefficient of friction and wear rate of hybrid composites. The optimal properties they observed for the addition of 2 % V and 1.5 % Gr.

Mortimer investigated the effect of vanadium carbide on the wettability between copper and carbon [11]. He tested the wetting angle using Cu-1 at.% V alloy at 1150 ℃ on carbon substrate. After 60 minutes of holding, the contact angle decreased to 68°. This is important for good gas pressure infiltration of graphite with molten copper.

Vanadium carbide (VC) can significantly influence interface bonding via enhanced adhesion between copper and graphite. This carbide could reduce the mismatch in the thermal expansion coefficients and mechanical properties between copper and graphite. It promotes the formation of strong chemical bonds at the interface, leading to better load transfer and overall mechanical performance of the composite. Thanks to this, the composites possess increased hardness and wear resistance as VC is a hard material. This makes the copper-graphite material more suitable for applications requiring high durability and a lower wear rate.

The creation of VC will also influence the thermal and electrical conductivity of the copper-graphite composite: While graphite and copper both have high thermal conductivities, the interface resistance can be reduced with VC. On the contrary, VC will slightly reduce the overall electrical conductivity of the composite due to its lower electrical conductivity compared to copper and graphite. Concerning tribological properties, VC further reduces the wear rate by providing a more stable and wear-resistant interface after creating a graphite-rich mixed layer on the surface [12]. VC can enhance the thermal stability of the interface, preventing degradation at high temperatures and enabling copper-graphite composite in high-temperature applications where copper and graphite might otherwise experience differential expansion and degradation.

Hence, this work aims to investigate the physical properties of the copper-graphite composite when vanadium is used as a carbide-forming element. The work is focused on determining microstructure and measuring the chosen thermophysical properties and hardness of the Cu-graphite composite prepared via gas pressure infiltration of mixed graphite powder with 1 vol.% of V powder with molten copper. Expected results are the creation of VC with high mechanical properties, low CTE, and reasonable thermal conductivity. The composite samples without vanadium were also prepared to compare microstructure and investigated properties.

2. Experimental

2.1. Materials and technology

Natural graphite powder was purchased from company KOH-I-NOOR GRAFIT s.r.o., Netolice, Czech Republic, with $d_{50} = 55.8$ μm and $d_{90} = 106.7$ μm (according to the supplier). The graphite powder underwent further sieving to attain a uniform particle size distribution, confining the particle size range between 63 and 125 microns. The graphite powder exhibited a characteristic flaky particle structure shown in Fig. 1a. Moreover, angular vanadium powder with a purity of 99.5 %, employed as a carbide-forming element from company MaTecK GmbH., Julich, Germany, was incorporated, with a maximum particle size not exceeding 75 microns (see Fig. 1b).

The composite samples were prepared via gas pressure infiltration of a powder mixture [13] of graphite and 1 vol.% of vanadium powder with molten copper (Cu-(C-1V)). Graphite and 1 vol.% vanadium powders were mixed using ethanol as a dispersant media and homogenized in a three-dimensional WAB Turbula Type T2F blender device (WILLY A. BACHOFEN AG, Muttenz, Switzerland) for 1 h to achieve a homo-

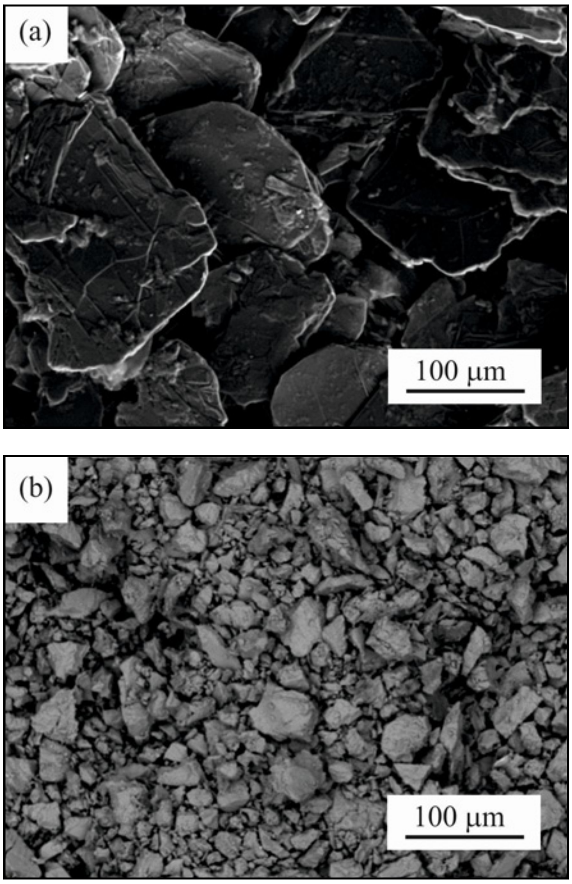

Fig. 1. Morphology of graphite (a) and vanadium (b) powders.

geneous distribution of the reinforcing phases. Then, the ethanol was evaporated at 90 ℃ for 2 h in the electric oven. The homogenized powder blend was placed in a crucible with a diameter of 18 mm and height of 19 mm and located at the bottom of a sealed vessel. Copper bars (high purity level of 99.9 %) 900 g in weight were located in the upper section of the vessel to allow for the subsequent melting of the copper. The autoclave (medium autoclave, IMMM SAS, Slovakia) was sealed, evacuated, and heated to 1250 ℃ with a heating rate of 20 ℃ min^{-1}. Copper was melted, and the melt was heated to 1250 ℃ and held there for 90 min. Afterward, the system was pressurized to 5 MPa for 5 min under a nitrogen atmosphere. After the chosen infiltration period, the infiltrated samples were cooled down to RT in the sealed vessel under nitrogen. The composite samples without vanadium (Cu-C) were also prepared to compare the properties using the same technology conditions.

Samples for further investigations were cut from the prepared composites using combinations of electric discharge and CNC machining, turning, or milling. The Archimedes principle was utilized to determine the densities (ρ) of the composite materials. From the densities, volume fractions of both V_m (copper matrix) and V_r (graphite + 1 vol.% of vanadium reinforcement) were determined according to the rules of the mixture (ROM). The volume fractions are determined using the densities of each used element ($\rho_\mathrm{cu} = 8.96\,\mathrm{cm}^{-3}$, $\rho_\mathrm{c} = 2.26\,\mathrm{cm}^{-3}$, and $\rho_\mathrm{v} = 6.11\,\mathrm{g\,cm}^{-3}$).

2.2. Characterization

Particle size distribution of both graphite and vanadium powders was analyzed in wet mode by Laser Particle Sizer Fritsch Analysette 22 (FRITSCH GmbH, Idar-Oberstein, Germany).

SEM&EDS were used to examine the powders and preliminary microstructure of composites. JEOL JSM 6610 (JEOL Ltd., Tokyo, Japan) model scanning electron microscopy (SEM) with Energy Dispersive X-ray spectroscopy (EDS) OI X-max 50 mm^2 were employed to obtain semi-quantitative elemental results of samples with and without vanadium.

JEOL cross-section polisher IB-19520CCP ion beam was used to remove the upper surface layer to observe a better copper-graphite interface via selective etching. An ion beam of 4.5 kV under argon gas was used for 3 h at 20 ℃.

Phase structures and chemical composition of prepared composites were analyzed using X-ray diffraction on Bruker AXS D4 Endeavor diffractometer (Bruker, Billerica, MA, USA) with Bragg-Brentano geometry and Cu Kα radiation at IP SAS, Bratislava.

Microstructural characterization of composite with 1 vol.% of vanadium was performed using a probe-corrected FEI/Thermofisher Scientific Titan Themis 300 (Thermo Fisher Scientific Inc., Waltham, MA, USA) transmission electron microscope in scanning mode (STEM) at a 200 kV accelerating voltage equipped with energy dispersive X-ray spectroscopy (EDS, SuperX detector). The probe convergence angle was set to 17.5 mrad for imaging applications; the corresponding probe current was measured at ~ 70 pA. Scanning micrographs were acquired simultaneously by 3 detectors, namely high angle annular dark field (HAADF), collection angle 101–200 mrad, annular dark field detector (ADF), collection angle 24–95 mrad and annular bright field detector (ABF) with collection angle set to 13–20 mrad. Investigated samples were prepared by mechanical thinning to a thickness of approximately 60 μm, followed by Ar beam ion milling. Ion milling was performed by PIPS II Model 695 (Gatan, Pleasanton, CA, USA) using an accelerating voltage of 2–4 keV and an angle of 3° to the surface from both sides.

The microhardness of the fabricated composite samples was quantitatively measured by employing a Zwick/Roell ZHVμMicro Vickers hardness tester (ZwickRoell, Ulm, Germany). The Vicker hardness measurement (MHV0.2) was carried out by applying

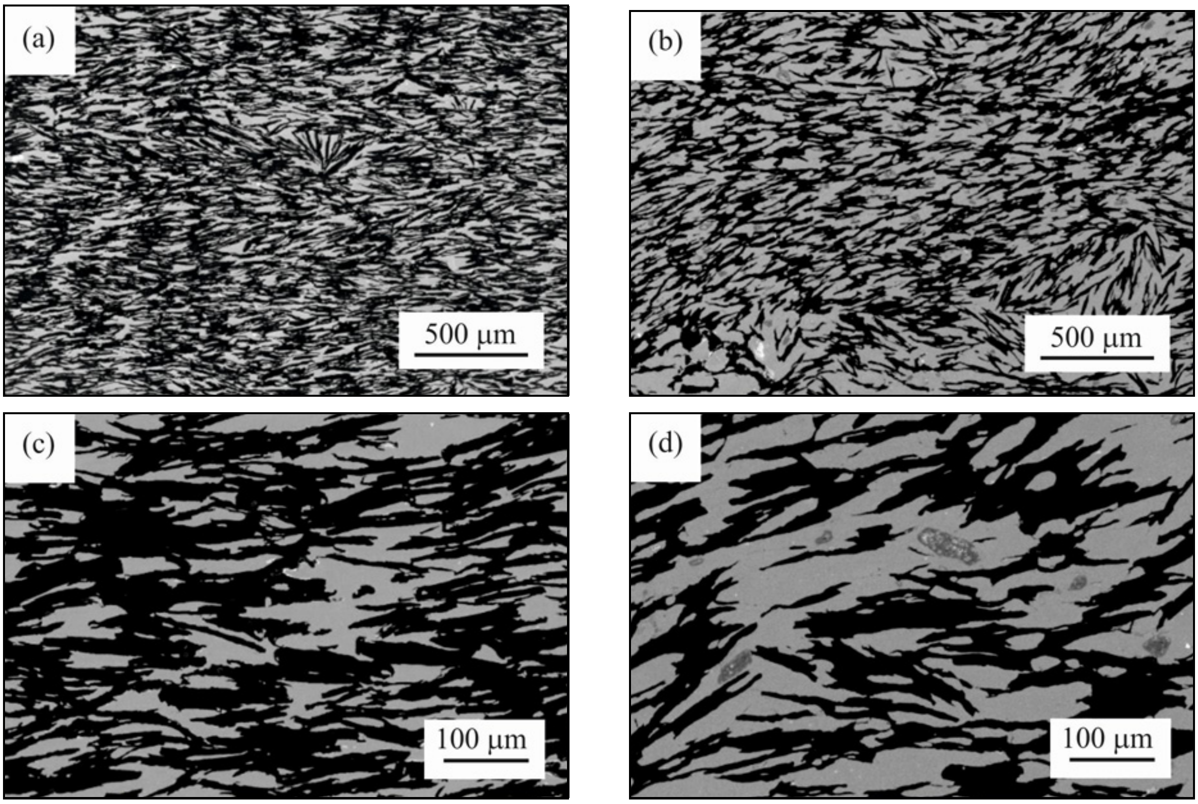

Fig. 2 Microstructure of prepared composite samples at different magnification: (a) Cu-C and (b) Cu-(C-1V) at 50×; (c) Cu-C and (d) Cu-(C-1V) at 200× (SEM).

a load of 200 gf (gram-force) for 10 s to form an indent on the sample's surface, as this method enables an accurate examination of the resistance of composites to deformation under specified conditions.

The thermal stability of composite materials was investigated using thermal expansion measurements (CTE). Cylindrical samples with dimensions of 4 mm in diameter and 5 mm in length were thermally cycled three to four times up to 800 ℃. The samples were heated at a rate of 3 ℃ min^{-1} and then cooled at 3 ℃ min^{-1} with an argon purge. The thermal cycling was conducted using a Linseis combined thermal analyzer L75/L81/2000 (Linseis, Selb, Germany) in dilatometer mode with an alumina holder. The first cycle was carried out to stabilize the geometry of the samples. The temperature ranged from 30 to 800 ℃ and afforded the capability to test how the materials responded to thermal stresses over a wide spectrum of temperatures.

From axial flow methods, a comparative cut bar method was used for the thermal conductivity measurement (ASTM E1225 Test Method) of samples [14]. Cylindrical samples are placed between two similar-sized cylinders with known thermal conductivity, consisting of two holes positioned for thermocouples as reference materials. If λ_R is the thermal conductivity of the references, then the thermal conductivity of the unknown sample λ_L is calculated as:

$$\lambda \frac{\Delta T_S}{L_S} = \lambda \frac{1}{2} \left(\frac{\Delta T_1}{L_1} + \frac{\Delta T_2}{L_2} \right), \quad (1)$$

where λ is the thermal conductivity of the S-sample, R-reference, and ΔT are temperature gradients at the sample, and reference R1 and R2.

3. Results

The graphite powder was sieved into the $63 < x \leq 125$ μm range in prior experiments. Therefore particle-size analysis was used to verify the sewing range of graphite powder and vanadium powder supplier's information. Graphite powder has $d_{50} = 91$ μm and $d_{90} = 157$ μm. Thanks to the flake shape of graphite, even larger powders could fall across the sieve of 125 μm. Vanadium powder has $d_{50} = 26.9$ μm and $d_{90} = 57$ μm, thus confirming supplier information that vanadium powder is below 75 μm.

3.1. Microstructure

Cu-C and Cu-(C-1V) composites SEM microstructure observations confirmed the overall isotropic orientation of graphite in prepared composites (Fig. 2). However, at small magnification, there are tiny local

T a b l e 1. Graphite and vanadium powder size distribution (μm)

Cumulative % point of diameter	Graphite	Vanadium
d_{10}	11.9 ± 10.4	10.1 ± 1.3
d_{50}	91.1 ± 2.7	26.9 ± 0.4
d_{90}	156.8 ± 2.9	57.4 ± 0.2

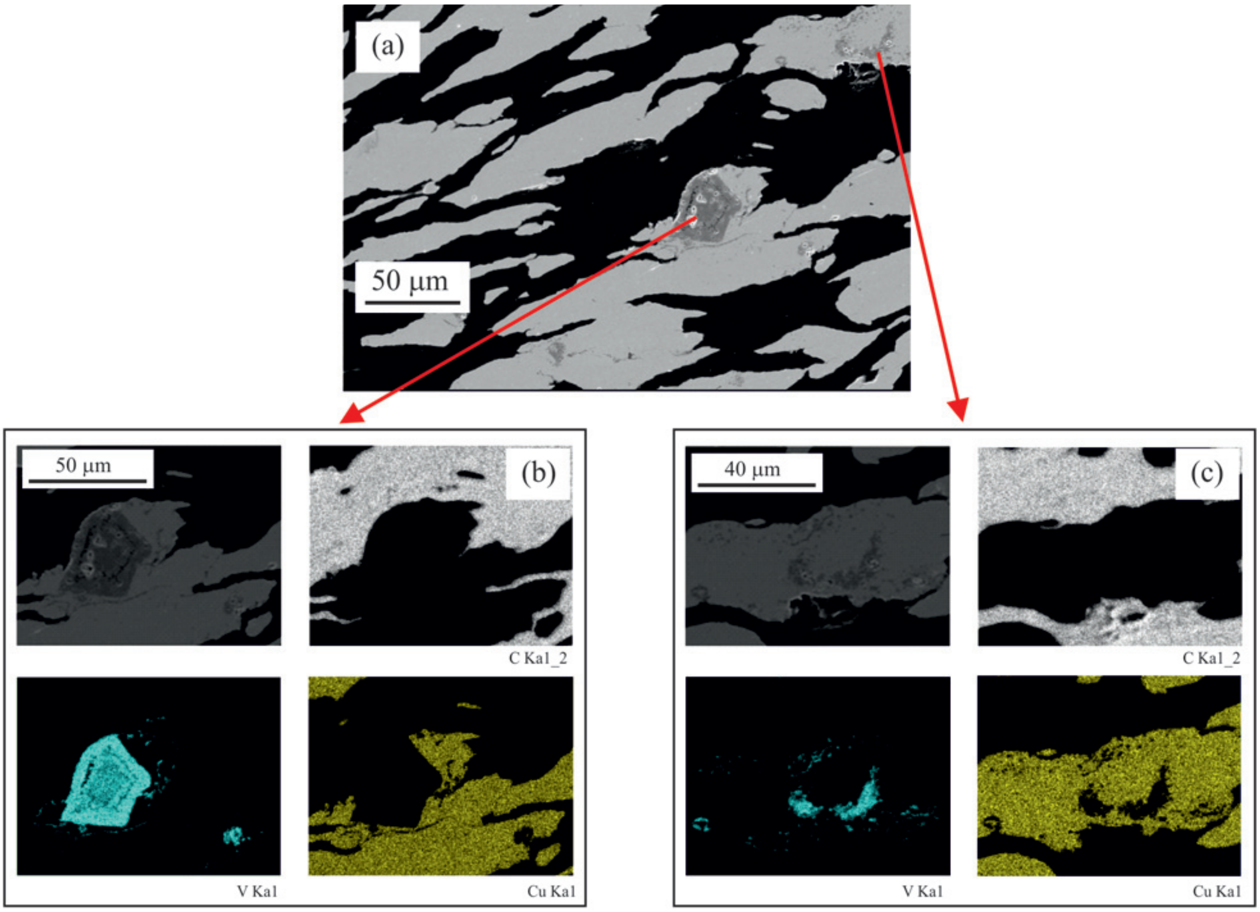

Fig. 3. Microstructure of Cu-(C-1V) (a) and corresponding area element analyses of certain grey phases present in the structure (b) and (c).

clusters of similarly oriented graphite flakes.

The porosity was not observed in the prepared Cu--C composite. Cu-C microstructure consists of black graphite and a light grey copper phase. In Cu-(C-1V) microstructure also, the dark grey phase up to 50 microns in size was observed (Fig. 2d). Small porosity-like holes inside the grey phase could be found (Figs. 3, 4). Element and point analyses indicate that the grey phase contains mostly vanadium (Figs. 3, 4), but graphite and copper were also observed inside this phase by EDS. This confirmed that vanadium carbide was created during infiltration.

The copper and graphite phases are thicker, and the distance between graphite clusters is larger when vanadium is used. It results from the changed wetting and spreading behavior of the copper when infiltrated between graphite powders when vanadium is present.

The vanadium-rich phase is entrapped in the copper or graphite surface. The grains of the vanadium-rich phase are often composed of clustered smaller grains (Figs. 3c and 4a) of around 10 μm in size and even less.

Some dark grey areas inside the copper phase have a size and angular shape similar to the used vanadium powder size and shape. Other areas have unclear morphology; they look like dissipated and/or partially solute angular vanadium powders into the copper phase (Figs. 3c, 4a).

The dark grey phase is also present at the copper--graphite interface, but there is no visible continuous

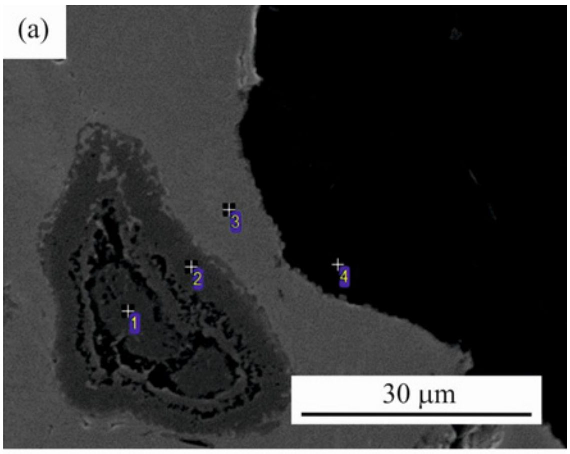

All results in atomic%

Spectrum	In stats.	C	V	Cu
1	Yes	28.50	70.18	1.32
2	Yes	53.15	46.85	
3	Yes	31.27		68.73
4	Yes	100.00		
Max		100.00	70.18	68.73
Min		28.50	46.85	1.32

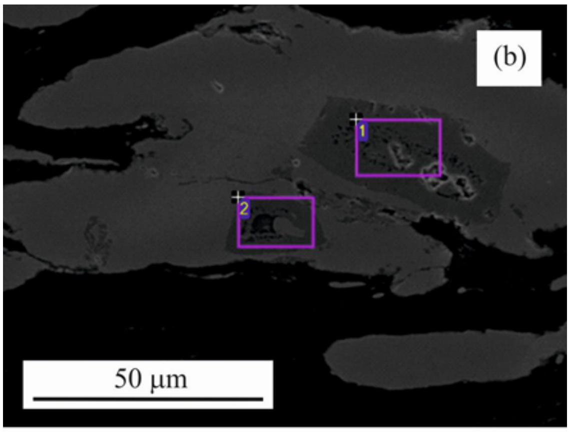

All results in weight%

Spectrum	In stats.	C	V	Cu	Total
1	Yes	19.57	80.29	0.15	100.00
2	Yes	18.33	54.56	27.10	100.00
Max		19.57	76.68	27.10	
Min		18.33	49.30	0.15	

Fig. 4. EDS point (a) and area (b) analyses of elements in Cu-(C-1V).

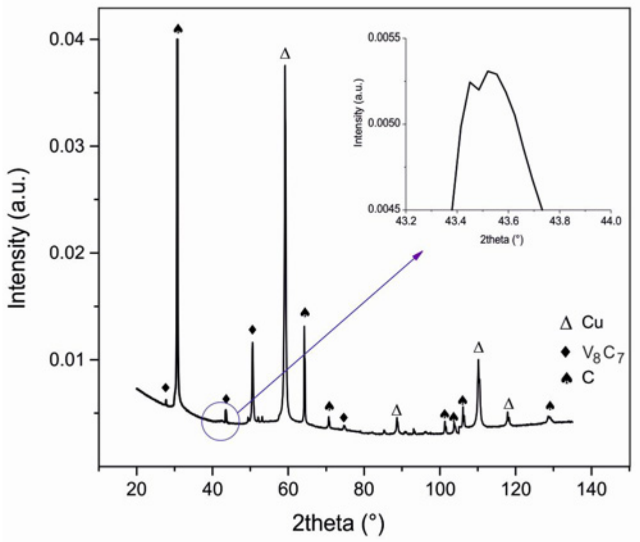

Fig. 5. X-ray diffraction spectra of Cu-(C-1V) with detail of doubled V_8C_7 (222) peak at 43.5°.

interface layer of the dark grey phase between flakes of graphite and the copper matrix. The dark grey phase covers graphite only partially, and this coverage is significantly below 50 % of the graphite surface.

The energy dispersive spectroscopy (EDS) results for vanadium and graphite show different at.% content ratios for them (Fig. 4): 50 at.% V:50 at.% C, 70 at.% V:30 at.% C, and 80 at.% V:20 at.% C were measured. Unfortunately, deciding which vanadium carbide was created is difficult – pure VC or VC_x, such as $VC_{0.875}$, $VC_{0.85}$, or $VC_{0.75}$. This is because the EDS technique is mostly a qualitative analysis technique. It could provide semi-quantitative results as well for heavy elements, but in the case of light elements (O, N, C), EDS couldn't give the 100 % correct quantitative result.

Therefore, to determine the precise composition of the dark grey phase in Cu-(C-1V), the composite X-ray diffraction (XRD) technique was used (Fig. 5). The X-ray diffraction spectra results detected peaks of graphite, copper, and V_8C_7 (or $VC_{0.875}$) vanadium carbide in macroscopic Cu-(C-1V) composite sample. V_8C_7 vanadium carbide is a non-stochiometric compound of carbon and vanadium.

Kurlov et al. [15] stated that ordered phase V_8C_7 is formed rather easily during high-temperature sintering of vanadium and carbon. The ordered phase is in the form of a superlattice. A superstructure is an upward extension of an existing structure above a baseline. In this case, the cubic vanadium structure is upward by interstitial carbon atoms and vacancies. Ordering in V_8C_7 is connected with the redistribution of carbon atoms and structural vacancies in the nonmetal sublattice sites. Further, they concluded that the degree of homogeneity of their initial powder is rather high, as was evidenced by the splitting of (220) peak at $2\theta = 63.2°$ corresponding to hkl planes 220 and 440. In the Cu-(C-1V) composite material, the splitting was observed for the V_8C_7 (222) peak at 43.5° (see detail at Fig. 5). In this case, it corresponds to hkl planes of 222 and 111. This confirms the high degree of homogeneity of prepared vanadium carbide during gas pressure infiltration.

Figure 6 shows the HRTEM EDS mapping of elements together with the high-angle dark field, dark field, and bright field picture of a single V_8C_7 carbide polycrystal attached to the graphite surface. The

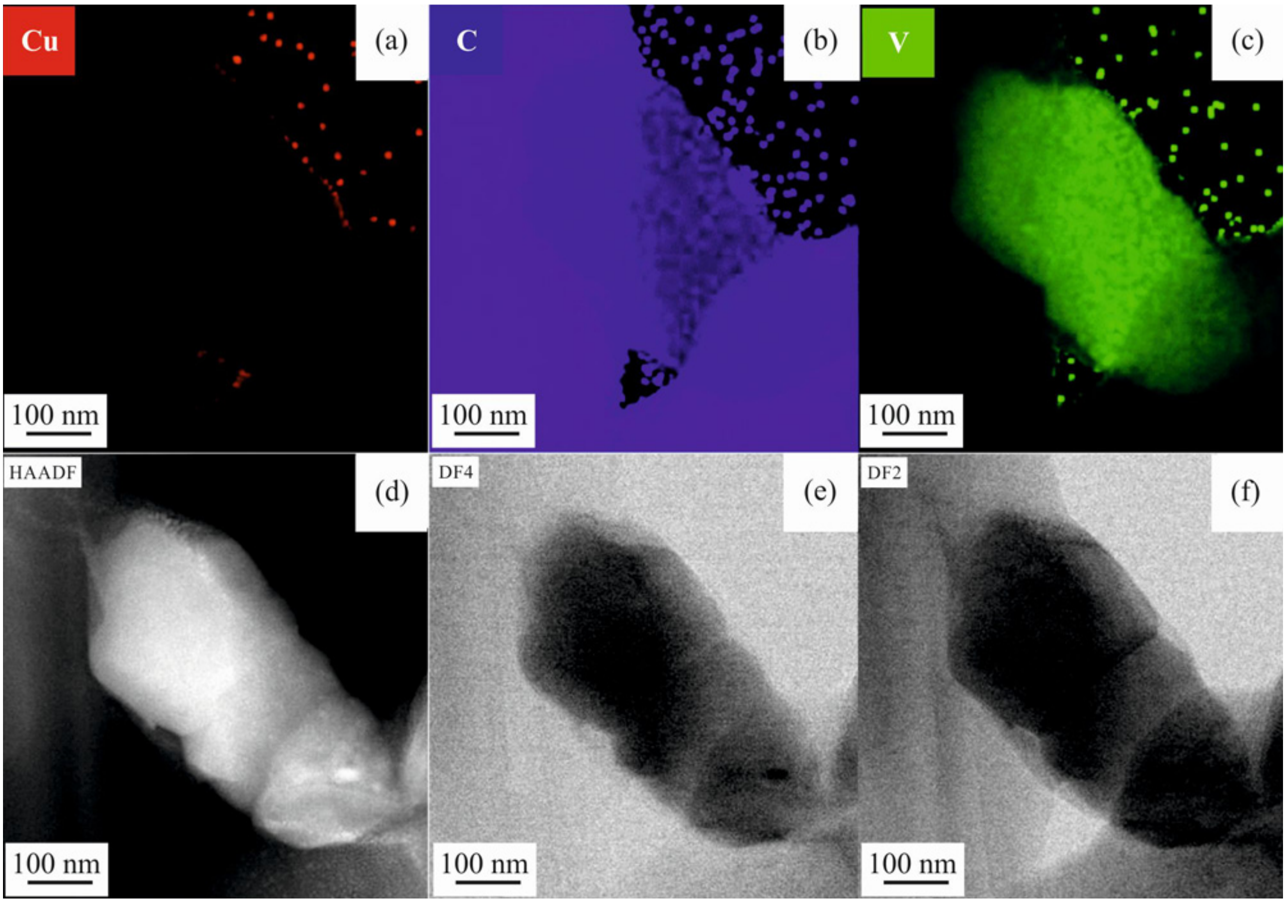

Fig. 6. HRTEM EDS mapping of elements (a) Cu, (b) C, (c) V and HRTEM, (d) high angle dark field, (e) dark field, and (f) bright field images of V_8C_7 attached to graphite interface in Cu-(C-1V) composite.

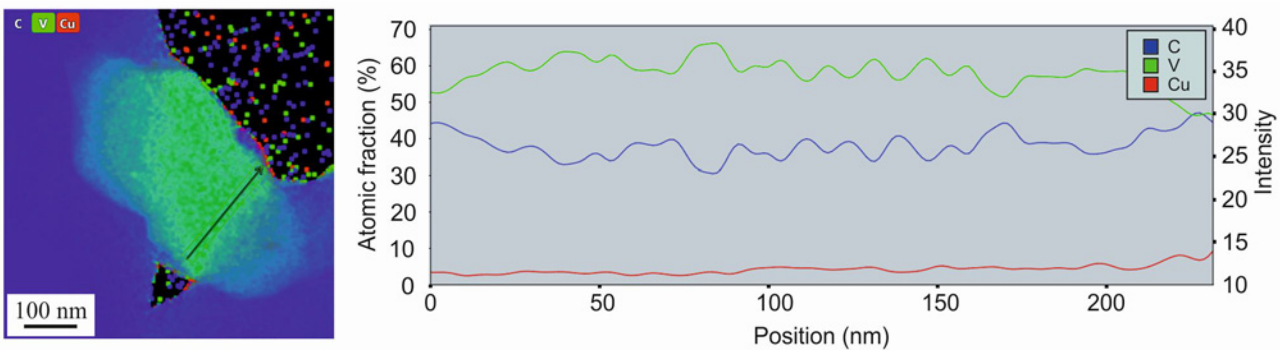

Fig. 7. HRTEM EDS line profile mapping of elements Cu-(C-1V).

characteristic size of the observed V_8C_7 polycrystal is 500 nm × 250 nm. Visible grain boundaries indicate that it consists of at least 3 smaller grains. Line element EDS analysis on HRTEM (Fig. 7) shows around 60 at.% of vanadium and 40 at.% of carbon inside.

HRTEM investigations also confirmed the presence of clusters of V_8C_7 crystals at the copper-graphite interface (Fig. 8). Usual size of polycrystals is again between 250–500 nm, and the length of vanadium carbide clusters is around 1 μm and more. Carbon, copper, and vanadium were found in interface spectral area analyses. V_8C_7 crystals have mostly sharp edges at the borders with copper regions. Line analysis indicates that in graphite, the diffusion interface is around 75 nm thick (Fig. 8c).

Finally, the vanadium carbide regions in a copper matrix of Cu-(C-1V) composite were also investigated: HRTEM diffraction investigations again confirmed the presence of V_8C_7 crystals. In this case, the size of V_8C_7 polycrystals varies between 500 nm–2 μm. They

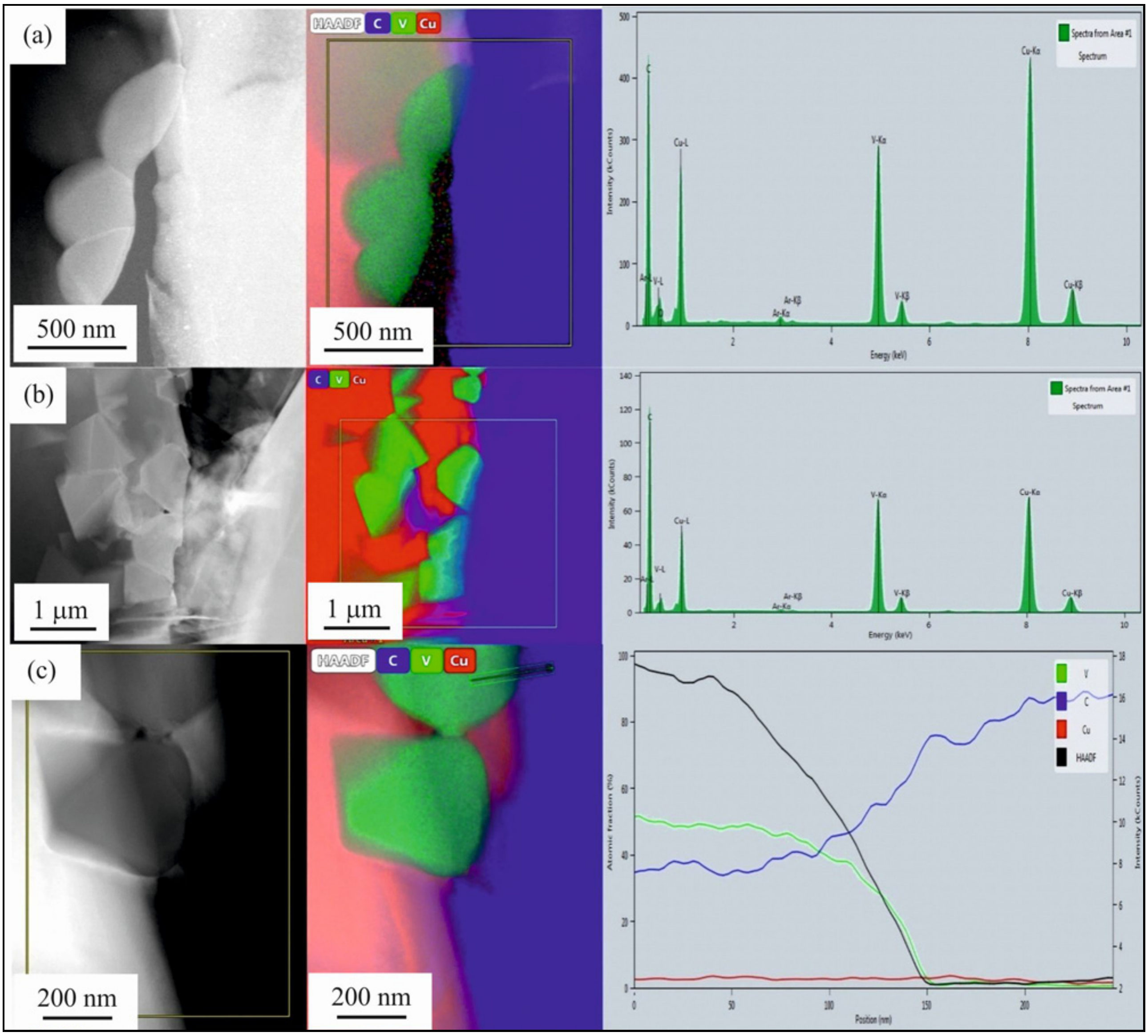

Fig. 8. HRTEM images of Cu-(C-1V) microstructure (a), (b) bright field, and (c) dark field images with corresponding energy spectra and line analysis of copper-graphite interface.

are surrounded on the left side (Fig. 9) by copper, and on the right side, carbon phase is present. Sharp borders with copper and diffusion borders with carbon were again distinguished. Computer identification of selected area diffraction patterns using *CrystalMaker Software* confirmed the V_8C_7 crystallographic superlattice structure. Fitted XRD data indicate the presence of cubic space group P4132 with an interatomic distance of 8.334 Å.

Summarizing, SEM, XRD, and HRTEM observations confirmed the reaction of carbon with vanadium. V_8C_7 carbide is created in cubic space group P4132 with an interatomic distance of 8.334 Å. It could be found on the copper-graphite interface with V_8C_7 phase size of 250–500 nm either as alone polycrystals or as polycrystals clusters. Inside the copper phase, clustered V_8C_7 crystals have a size of around 0.5–2 μm. There is almost a sharp transition between the copper and V_8C_7 phases. In the case of the graphite-V_8C_7 interface, the diffusion layer is around 75 nm thick.

3.2. Thermal properties and hardness

Thermal properties (thermal conductivity and coefficient of thermal expansion) and hardness were determined for the prepared composites (Table 2). The volume fractions of copper were calculated from the densities of used compounds ($\rho_{cu} = 8.96\ \mathrm{g\,cm^{-3}}$, $\rho_c = 2.26\ \mathrm{g\,cm^{-3}}$, and $\rho_v = 6.11\ \mathrm{g\,cm^{-3}}$) via the rule of mixture and area fraction determined using *ImageJ software*.

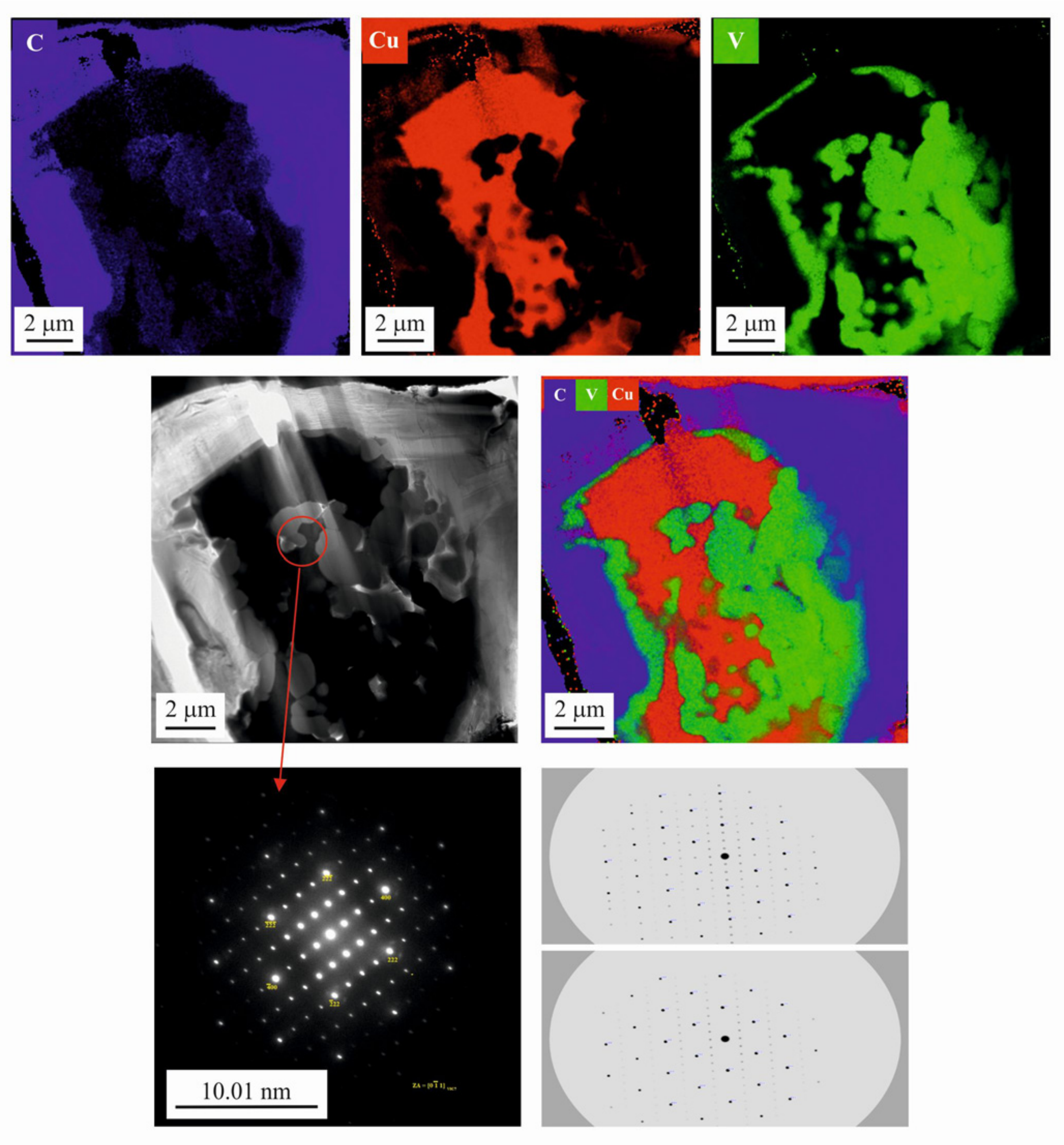

Fig. 9. HRTEM EDS elements maps, HRTEM dark field image of Cu-(C-1V) composite, combined elements map, selected area diffraction and corresponding V_8C_7 diffraction crystallographic model.

Table 2. Thermal properties and hardness of investigated composites

Sample	ρ (g cm^{-3})	Vcu (%)	TC (W m^{-1}K^{-1})	MHV0.2 (–)	CTE (10^{-6} K^{-1})
Cu-C	4.833	38.4	206.8	16.9 ± 0.8	7
Cu-(C-1V)	4.719	36.3	49.9	17.7 ± 2.2	10

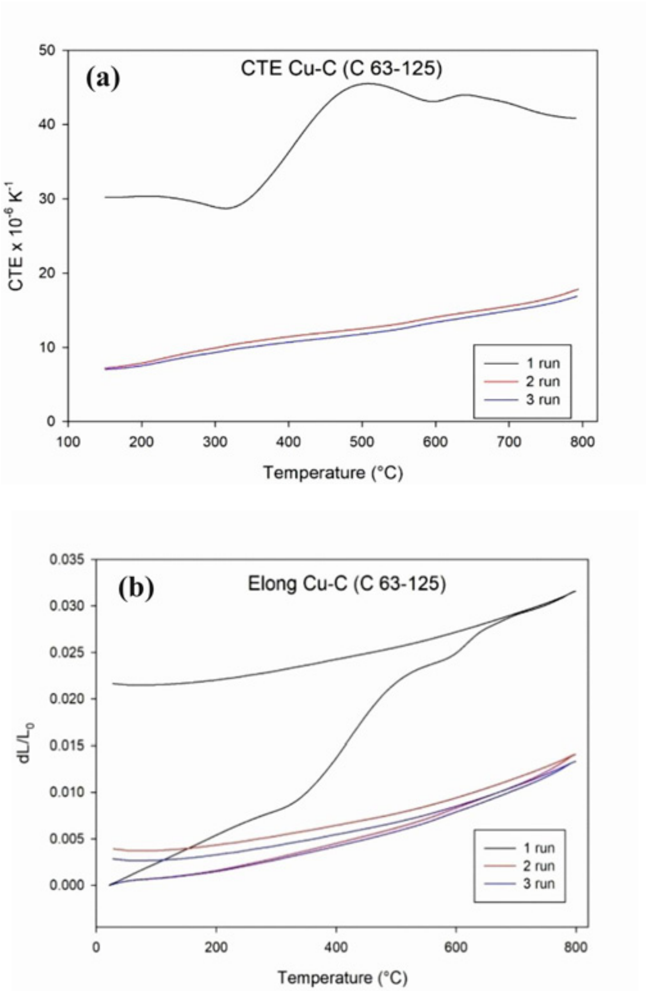

Fig. 10. Thermal expansion properties of Cu-C during 3 cycles: (a) CTE and (b) elongation.

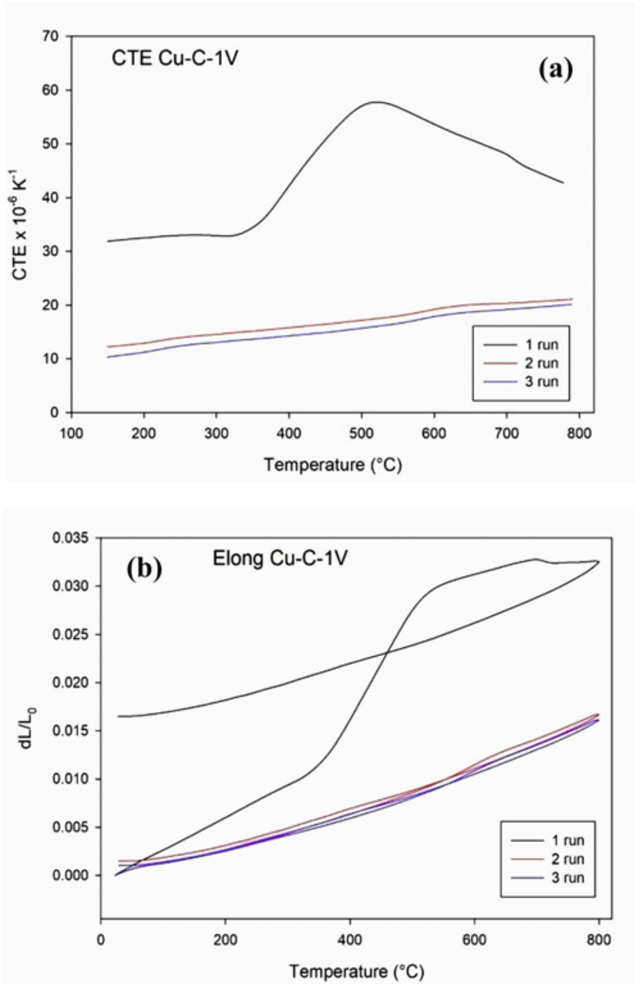

Fig. 11. Thermal expansion properties of Cu-(C-1V) during 3 cycles: (a) CTE and (b) elongation.

Vickers microhardness MHV0.2 tests were performed on polished cross sections of investigated composites used for SEM investigations: 15 measurements were performed, and average values with standard deviations were calculated. Introducing vanadium into the Cu-C structure increased MHV0.2 hardness from 16.9 to 17.7.

On the contrary, the thermal conductivity of Cu-(C-1V), as measured by the steady-state method composite, significantly decreased compared to pure composite without vanadium. The creation of V_8C_7 vanadium carbide is probably the reason for this result.

The thermal expansion coefficient (a) and elongation (b) of the copper-graphite composite as a function of the temperature in the range of 100–800 ℃ were measured (Fig. 10). Measurements were performed for 3 subsequent runs from 100 to 800 ℃ and cooling down to 100 ℃. During the first run, the sample geometry was stabilized. Then, the CTE of the Cu-C composite increases with temperature. CTE at 150 ℃ is $7 \times 10^{-6}\,\mathrm{K}^{-1}$.

Similar results were observed for the thermal properties of the Cu-(C-1V) composite. After 1st run, the thermal expansion graph shows expansion linearly increased with the temperature. CTE at 150 ℃ is $10.3 \times 10^{-6}\,\mathrm{K}^{-1}$ (Fig. 11).

The temperature changes in CTE and Cu-(C-1V) composite elongations are higher than in the Cu-C composite. On the other hand, permanent elongation after runs is higher for pure Cu-C composite.

It could be stated that vanadium has a considerable effect on the thermal expansion of the material and the elongation as well: the higher change in thermal expansion and elongation in Cu-(C-1V) may imply that vanadium introduces additional internal stresses on the crystalline level and changes also the way Cu interacts with graphite reinforcements.

4. Discussion

4.1. Microstructure

In this work, V_8C_7 carbide was prepared by gas pressure infiltration of the mixture of graphite with 1 vol.% of vanadium with molten copper at 1250 ℃. The carbide was found on the copper-graphite interface and inside the copper matrix.

At the beginning of the infiltration process, the powders of graphite and vanadium are in touch under the vacuum. With increasing temperature, they start to react in contact points. The reaction process is driven by the diffusion in crystalline solids.

Powers and Doyle [16] observed diffusion in a vanadium-carbon solid mixture. They found that the carbon is diffusing into vanadium and proposed the following equation to describe the temperature dependence of the diffusion coefficient of carbon into vanadium $D_{\text{C-V}}$ (Eq. (2)):

$$D_{\text{C-V}} = 0.0047 \exp(-27300/RT), \qquad (2)$$

where diffusion coefficient $D_{\text{C-V}}$ is in $\text{cm}^2\,\text{s}^{-1}$, T is the absolute temperature in K, and $R = 8.31446\,\text{J}\,\text{mol}^{-1}\,\text{K}^{-1}$ is the universal gas constant. At the melting temperature of copper (1353 K), the $D_{\text{C-V}}$ is $0.000415\,\text{cm}^2\,\text{s}^{-1}$.

According to Bird and Stewart [17], the diffusion distance (x) at the time (t) for carbon diffusion into vanadium could be calculated using the following equation:

$$x = 2\sqrt{(D_{\text{C-V}}t)}. \qquad (3)$$

Powder size analysis confirmed that the used vanadium powder size is smaller than 75 microns. Using Eq. (3), this distance is in 0.034 s diffused by carbon at 1353 K. Of course, in reality, it probably takes a longer time due to imperfect contacts, but the powder mixture is held together with copper melt at 1250 ℃ for 90 min prior 5 MPa pressure is applied. Therefore, it could be expected that all vanadium in contact with graphite powders reacted with carbon atoms before infiltration.

A very small amount of vanadium powders could be in contact only with other vanadium powders. In that case, the diffusion of carbon across powder surfaces could be significantly slowed, and such vanadium powders could be intact for a long time and could react with copper melt during infiltration.

Summarizing, the creation of vanadium carbide is a rapid process realized via interstitial solid diffusion of light carbon atoms into vacancies in a vanadium body-centered cubic structure.

According to Okamoto [18], on the carbon-rich side of the V-C binary diagram, the possible phases that could be created are VC at 37.1–47 at.% of carbon, V_6C_5 at 42–46 at.% of carbon, and V_8C_7 at 46.7 at.% of carbon. The mixture of V_8C_7 with carbon coexists above 46.7 at.% of carbon.

Chong et al. [19] calculated the Gibbs free energy of V_8C_7 and showed that it is smaller than that of VC. They also suggest that the V_8C_7 is more stable at high temperatures and easier to form than VC. On the contrary, Chong et al. [20] also calculated the formation enthalpy of various other carbides and concluded that V_6C_5 (–0.541 eV per atom) has the lowest value of formation enthalpy, indicating V_6C_5 as the most stable phase inside the V–C binary compounds. Moreover, they observed that the formation enthalpy of V_8C_7 (–0.522 eV per atom) is lower than that of VC (–0.405 eV per atom), confirming the higher stability of V_8C_7 carbide.

Bin Wang et al. [21] calculated that the increase in the absolute values of formation energies and cohesive energies follows the order V_4C_3, VC, and V_8C_7, which indicates that the C vacancy decreases the stability of VC, but due to the difference in symmetry (VC is Fm3m and V_8C_7 is $P4_332$), V_8C_7 is more stable than VC.

When the infiltration pressure is applied, the molten copper is driven into the powder mixture. The composite is prepared by cooling powders inside molten metal under external pressure until the copper matrix becomes solid. This external energy and type of cooling is probably responsible for why the V_8C_7 phase is observed after cooling down to room temperature in prepared composite rather than VC or V_6C_5 carbide.

Preparation of the V_8C_7 phase from vanadium and carbon powder mixtures is not unusual and was observed by various researchers: Amaral et al. [22] prepared vanadium carbides from the mixture of vanadium and carbon powders in the solar furnace and for comparison in an electric furnace under an argon and nitrogen atmosphere. They used powders of V (< 45 μm) and carbon powders (either Gr (< 50 μm) or aC (charcoal activated carbon)). The mole ratio of C/V in the starting powder mixture was fixed to be 1.5 to ensure the presence of free carbon coexisting with the reaction product at the end of the reaction. They found that the XRD peak positions of any examined specimen were comparable and coincided with that for $VC_{0.88}$, implying that the formed compounds were all carbide of the phase V_8C_7. Hou et al. observed that due to a significantly higher concentration of graphite [23], V_8C_7 tends to be created after cooling the composite created by the floating zone technique down to room temperature.

Vanadium has a body-centered cubic (bcc) structure with $a = 303$ pm [24]. HRTEM results at Figs. 6–8 indicate that V_8C_7 polycrystals of 200 nm–1 μm size were created. During infiltration, the rearrangement

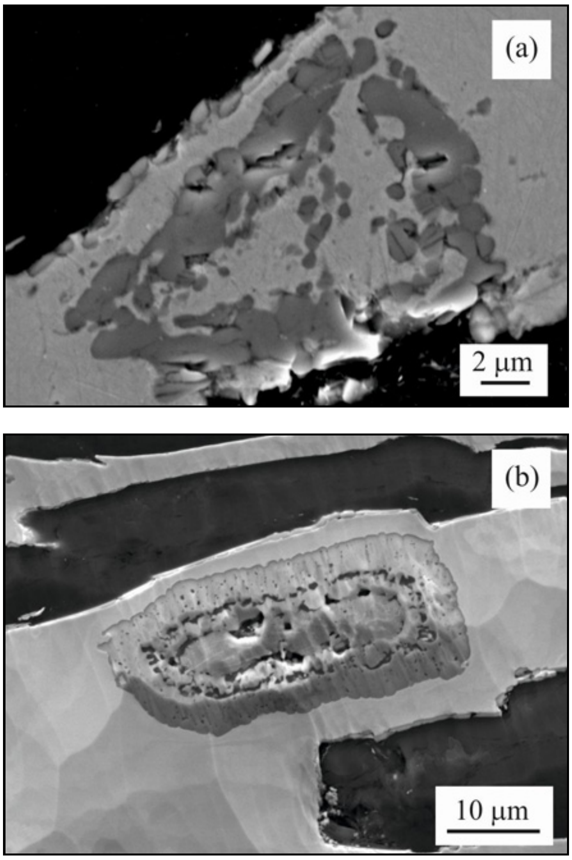

Fig. 12. V_8C_7 clusters (dark grey) in copper matrix (light grey) surrounded by black graphite phase – microstructures without and after ion etching (SEM).

of the previous bcc vanadium structure with a = 303 pm to cubic space group P4132 with a = 833.4 pm [25], according to XRD results, took place. This indicates that volumetric changes and minimization of surface-to-volume energy probably created polycrystal agglomerates inside the volume of original vanadium particles. Small voids, cracks, and pores are also present (Fig. 12).

During the infiltration, the copper is probably forced to flow into these cracks and voids. Copper subsequently erodes the V_8C_7 crystals via the voids and cracks at the grain boundaries of graphite with vanadium carbide. Due to external pressure, some particles are detached from the graphite surface.

Thanks to the different densities of copper and vanadium carbide, Pascal law, Archimedes law, and Brownian motion, vanadium carbide particles move inside copper melt. The molten copper erodes V_8C_7 phase into smaller grains of 1–5 microns (Fig. 12) and even smaller, as indicated by TEM results. After cooling, the V_8C_7 dark grey phase deep inside the copper matrix is produced, significantly dissipated into small polycrystals.

Another possibility is the vanadium reaction with copper. However, vanadium has very small solubility in copper: At and above peritectic temperature (1120 ℃) the maximum solubility of vanadium does not exceed 0.2 at.% [24].

Summarizing: V_8C_7 carbide was created by rapid carbon diffusion to solid vanadium at high temperatures. In a short time, vanadium powder transformed into clusters of V_8C_7-sized polycrystals with voids, cracks, and pores between them due to volumetric changes in the crystallographic structure. Later, copper melt infiltrates them. Molten copper tears apart the V_8C_7 clusters, even those connected to the graphite phase. The Pascal law, Archimedes law, and Brownian motion further disperse the clusters and agglomerates into smaller pieces and force them to move in the copper phase.

4.2. Hardness

The hardness of copper-graphite composites is important for their application in sliding contacts. Higher hardness usually leads to a lower wear rate. The hardness of copper-graphite composites is influenced by several factors other than the graphite content: the size and shape of the graphite particles, degree of graphitization, processing methods, and presence of various additives or copper coating on graphite (see Table 3).

At low graphite content [26–28], high hardness values are observed at 35–55 MHV for copper-graphite composites prepared by spark plasma sintering (SPS) and other powder metallurgical methods (PM). The hardness measured in this work (at 61 vol.% graphite) is 16.9 ± 0.8 MHV. Due to higher graphite content, it is significantly lower than that originating from the research mentioned above.

Xu Jiang et al. produced via powder metallurgy composites with both natural graphite and copper powders of the same size (~ 40 μm) [29]. The final composite has 16 wt.% C, 1 wt.% SiO_2 and 83 wt.% Cu composition. It is around 43 vol.% of graphite. The hardness of this composite is 12 MHV and is lower when compared with the investigated Cu-C composites.

Adding 1 vol.% of vanadium into the composite and creating V_8C_7 carbide slightly increases the Vickers hardness of the composite compared with the non-reinforced one (Table 3) up to 17.7 ± 2.2 MHV. This is the result of the high hardness of V_8C_7 carbide. Bin Wang et al. found a value of 22.8 GPa (2325 HV after recalculation) for dense carbide [30]. The results are in qualitative agreement with the results of Jabinth et al. [10]. They observed that Cu-V-Gr composites prepared by the stir casting process enhanced HRB hardness from 62 for pure copper to 95 for Cu-2V-1.5Gr.

It could be summarized that due to high graphite

Table 3. Hardness results of copper-graphite composites prepared by various technologies

Sample	Production method	MHV0.2 (–)	Reference
Cu-2.5 wt.% C	SPS	54.8	[26]
Cu-10 wt.% C (50 wt.% Cu coated)	Hot press sintering	35.65	[27]
Cu-16 wt.%C-1 wt.% SiO_2	PM	12	[29]
Cu- 6 wt.% C	PM	38.93	[28]
Cu-C	GPI	16.9 ± 0.8	This work
Cu-(C-1V)	GPI	17.7 ± 2.2	This work

Table 4. Thermal conductivity of copper-graphite composites prepared by various technologies

Sample	Production method	Thermal conductivity ($W\,m^{-1}\,K^{-1}$) (X-Y)	Thermal conductivity ($W\,m^{-1}\,K^{-1}$) (Z)	Reference
Cu-50 vol.% C	Hot press sintering	678.6	57.3	[32]
Cu-50 vol.% C	PM	124.5	124.5	[31]
Cu-60 vol.% C	PM	~ 599	54	[33]
Cu-60 vol.% C	Hot press sintering	~ 600	~ 40	[34]
Cu-61 vol.% C	SPS	~ 531	74	[35]
Cu-61.6 vol.% C	GPI	206.8	206.8	This work
Cu-63.7 vol.% C (C-1V)	GPI	49.9	49.9	This work
Cu-70 vol.% C	Vacuum hot press	–	110	[36]
Cu-72.08 vol.%C	SPS	~ 600	~ 39	[37]
Cu-72.08 vol.%C	PM	~ 470	40	[38]

content, the hardness of investigated composites is relatively low, 16.9 MHV, but comparable to similar results in scientific literature. Adding 1 vol.% of vanadium and creating a hard V_8C_7 phase increases the final hardness of the composite to 17.7 MHV due to the presence of a hard carbide phase.

4.3. Thermal properties

The thermal conductivity and coefficient of thermal expansion of copper-graphite composites are crucial properties that influence composites utilization in many areas, such as electronics, heat sinks, and sliding materials [31]. Due to the fact that graphite has a hexagonal crystal lattice, its thermal conductivity and coefficient of thermal expansion are anisotropic concerning the basal plane (a direction or X-Y) and perpendicular to the basal plane (c direction or Z plane). Graphite flakes are often oriented with a Z plane parallel to the applied load, depending on the preparation method. This leads to significant anisotropy of copper-graphite composites (Tables 4, 5).

While in-plane X-Y thermal conductivity of graphite can reach as high as 1000 $W\,m^{-1}\,K^{-1}$ [39], Z plane thermal conductivity is only around 38 $W\,m^{-1}\,K^{-1}$ [40]. On the other hand, copper has a value of about 400 $W\,m^{-1}\,K^{-1}$ [41]. Table 4 compares thermal conductivity results for copper-graphite composites prepared by various production methods. Thermal conductivity values are within specific graphite and copper values and vary according to the anisotropy of the composite microstructure.

The microstructure of investigated composites is mostly isotropic and homogeneous on a macro scale. Therefore, it is not possible to distinguish X-Y and Z planes (see Fig. 2). Thermal conductivity 206.8 $W\,m^{-1}\,K^{-1}$ observed for Cu-C composites in this work is lower than the best results in the X-Y plane, but due to random orientation of graphite flakes (Fig. 2), they are the best in Z plane at 61 vol.% of graphite.

Adding vanadium decreases thermal conductivity significantly. Even 1 vol.% on the interface between copper and graphite decreases thermal conductivity from 206.8 down to 49.9 $W\,m^{-1}\,K^{-1}$. The thermal conductivity of vanadium carbide plays a significant role in this case: Wei Li et al. [42] consolidated V_8C_7 carbide powder specimens up to a wide range of final densities (57.5–84.3 %) and observed thermal conductivity in the range of 7.5–15 $W\,m^{-1}\,K^{-1}$ at 100 °C. They also concluded that they are significantly lower than the expected value for dense V_8C_7 carbide 39 $W\,m^{-1}\,K^{-1}$.

Yang Lin et al. [43] calculated the thermal conductivity of V_8C_7 24.5 $W\,m^{-1}\,K^{-1}$ at 300 K and 25.7 $W\,m^{-1}\,K^{-1}$ at 1600 K. They concluded that thermal conductivity increases with temperature and decreases with carbon vacancy. They also observed that electron conductivity dominates the thermal conductivity of V_8C_7. Phonon conductivity is only 3 % of

Table 5. Coefficients of thermal expansion of copper-graphite composites prepared by various technologies at high graphite concentrations

Sample	Production method	Thermal expansion 10^{-6} K^{-1} (Z)	Thermal expansion 10^{-6} K^{-1} (X-Y)	Reference
Cu-50 vol.% C	Hot press sintering	~ 14.5	~ 9 (150C)	[34]
Cu-50 vol.% C	PM	9.8	3.2	[33]
Cu-50 vol.% C	PM	11.73	10.41	[44]
Cu- 50 vol.% C	PM	–	6.9	[45]
Cu-60 vol% C	PM	~ 17 (150C)	~ 4 (150C)	[46]
Cu-61 vol.% C	SPS	6.2	–	[35]
Cu-61.6 vol.% C	GPI	7	7	This work
Cu-63.7 vol.% (C-1V)	GPI	10	10	This work
Cu-72.08 vol.% C	SPS	6.6	–	[37]
Cu-72.08 vol.% C (62 μm)	PM	14	~ 6	[38]

total thermal conductivity in V_8C_7.

It can be summarized that the electron conductivity of V_8C_7 prevents the exchange of energy between copper-free electrons and vibrations of graphite structure phonons even more as it is in the simple copper-graphite composite. Therefore, the thermal conductivity of the Cu-(C-1V) composite is significantly small and almost comparable to the thermal conductivity of graphite. It looks like a total switch-off of the graphite phase from composite thermal conductivity. Moreover, due to the possible very small solubility of vanadium in copper, diminished thermal conductivity of the copper matrix could also play some role in this low value of observed thermal conductivity.

Table 5 compares coefficients of thermal expansion for copper-graphite composites prepared by various production methods. The coefficient of thermal expansion of graphite flakes is significantly anisotropic. X-Y plane has a value of -1.5×10^{-6} K^{-1} [40], and in the Z plane, 28×10^{-6} K^{-1} [47]. The coefficient of thermal expansion of pure copper is around 16–17 $\times 10^{-6}$ K^{-1} [41].

The coefficient of thermal expansion of the investigated Cu-C composite (7×10^{-6} K^{-1}) is close to the average values in the X-Y plane results in the scientific literature; and 6.81×10^{-6} K^{-1}. Cu-(C-1V) value 10×10^{-6} K^{-1} is comparable to the average in Z plane results 11.3×10^{-6} K^{-1}.

Chong et al. [48] calculated the coefficient of thermal expansion of V_8C_7 in the range of 6–10 $\times 10^{-6}$ K^{-1}. The addition of vanadium into the copper-graphite composite and the creation of the V_8C_7 phase resulted in the increase of the coefficient of thermal expansion up to 10×10^{-6} K^{-1}.

5. Conclusions

Copper graphite composite with 1 vol.% of vanadium was prepared using gas pressure infiltration of graphite-vanadium powder mixture with molten copper. Composite contains 63.7 vol.% of graphite. For comparison, Cu-C composite without vanadium with a similar volume fraction of graphite (61.6 vol.%) was also prepared. The obtained results are:

– Almost 100 % theoretical density was achieved.

– Microstructure observations confirmed the isotropic orientation of the graphite phase in prepared composites.

– The copper and graphite phases are thicker, and graphite clusters distance is larger when vanadium is used.

– XRD and HRTEM observations confirmed that V_8C_7 carbide was created. V_8C_7 carbide was created by the solid diffusion of carbon atoms into vanadium powders.

– Molten copper tore apart the V_8C_7 clusters. The Pascal law, Archimedes law, and Brownian motion further dispersed the clusters and agglomerates into smaller ones.

– There is a sharp transition between the copper and V_8C_7 phases. The diffusion layer at the borders of graphite-V_8C_7 is around 75 nm thick.

– Clusters of V_8C_7 polycrystals were found on the copper-graphite interface with size of 250–500 nm; dissipated polycrystals were also found within copper with size of 0.5 – 1 μm.

– The hard V_8C_7 phase increased the hardness of the composite to 17.7 MHV from the value of 16.9 MHV for pure copper-graphite composite.

– The thermal conductivity of copper-graphite composite is 206.8 W m^{-1} K^{-1}. The creation of the V_8C_7 phase resulted in a low thermal conductivity of 49.9 W m^{-1} K^{-1}.

– Coefficients of thermal expansion of prepared composites are 7×10^{-6} K^{-1} for Cu-C and 10×10^{-6} K^{-1} for Cu-(C-1V). The addition of vanadium increases CTE by 43 %.

It could be concluded that in the case of gas pressure infiltration, the addition of vanadium powder led to decreased effective thermal conductivity of the copper-graphite composite. Created V_8C_7 carbide increased the hardness and coefficient of thermal expansion of the prepared composite.

Therefore, vanadium addition is not attractive for Cu-graphite composite industrial applications that require good thermophysical properties.

Acknowledgements

This research was funded by a PhD grant from the Slovak Academy of Sciences project No. 1907 (Project: "Changes in the interface microstructure of copper-based composite materials with a carbon skeleton prepared by gas pressure infiltration"). This research was also partially supported by the VEGA project: Laser surface modification of Ti-TiB_2 biocomposites prepared by powder metallurgy process in order to increase their osseointegration (VEGA 2/0054/23).

The authors thank Dr. Juraj Lapin† (In memoriam) for the proposal of this research topic. They also thank Dr. Peter Svec and Dr. Peter Svec Jr. from IP SAS, Bratislava, for their valuable help with XRD and HRTEM analyses.

References

[1] C. Samal, J. S. Parihar, D. Chaira, The effect of milling and sintering techniques on mechanical properties of Cu-graphite metal matrix composite prepared by powder metallurgy route, J. Alloys Compd. 569 (2013) 95–101. https://doi.org/10.1016/j.jallcom.2013.03.122
[2] H. Wang, Z. Tao, X. Li, X. Yan, Z. Liu, Q. Guo, Graphite fiber/copper composites prepared by spontaneous infiltration, Appl. Surf. Sci. 439 (2018) 488–493. https://doi.org/10.1016/j.apsusc.2018.01.035
[3] W. Wei, X. Li, Z. Yang, Z. Huang, H. Zuo, Q. Liao, W. Xie, G. Yin, G. Wu, Highly conductive graphite matrix/copper composites by a pressureless infiltration method, J. Appl. Phys. 130 (2021) 015102. https://doi.org/10.1063/5.0056198
[4] A. Jamwal, P. Prakash, D. Kumar, N. Singh, K. K. Sadasivuni, H. Kumar, K. Harshit, S. Gupta, P. Gupta, Microstructure, wear and corrosion characteristics of Cu matrix reinforced SiC-graphite hybrid composites, J. Compos. Mater. 53 (2019) 2545–2553. https://doi.org/10.1177/0021998319832961
[5] R. Zhang, X. He, H. Chen, X. Qu, Effect of alloying element Zr on the microstructure and properties of graphite flake/Cu composites fabricated by vacuum hot pressing, J. Alloys Compd. 770 (2019) 267–275. https://doi.org/10.1016/j.jallcom.2018.08.107
[6] H. Zuo, W. Wei, X. Li, Z. Yang, Q. Liao, Y. J. Xian, G. Wu, Enhanced wetting and properties of carbon/copper composites by Cu-Fe alloying, Compos. Interfaces 29 (2021) 111–120. https://doi.org/10.1080/09276440.2021.1904720
[7] C. R. Rambo, N. Travitzky, P. Greil, Conductive TiC/Ti–Cu/C composites fabricated by Ti–Cu alloy reactive infiltration into 3D-printed carbon performs, J. Compos. Mater. 49 (2015) 1971–1976. https://doi.org/10.1177/0021998314541307
[8] P. Xiao, Y. H. Lu, Y. Z. Liu, Z. Li, H. C. Fang, W. Zhou, R. S. M. Almeida, Y. Li, Microstructure and properties of Cu-Ti alloy infiltrated chopped Cf reinforced ceramics composites, Ceram. Int. 43 (2017) 16628–16637. https://doi.org/10.1016/j.ceramint.2017.09.053
[9] H. Zuo, W. Wei, Z. Yang, X. Li, J. Ren, Y. Xian, Q. Liao, G. Yin, G. Gao, G. Wu, Performance enhancement of carbon/copper composites based on boron doping, J. Alloys Compd. 876 (2021) 160213. https://doi.org/10.1016/j.jallcom.2021.160213
[10] J. Jabinth, N. Selvakumar, Enhancing the mechanical, wear behaviour of copper matrix composite with 2V-Gr as reinforcement, Proceedings of the Institution of Mechanical Engineers, Part J: Journal of Engineering Tribology 235 (2021) 1405–1419. https://doi.org/10.1177/1350650120960573
[11] D. A. Mortimer, M. Nicholas, The wetting of carbon by copper and copper alloys, J. Mater. Sci. 5 (1970) 149–155. https://doi.org/10.1007/BF00554633
[12] J. Kováčik, Š. Emmer, J. Bielek, Ľ. Keleši, Effect of composition on friction coefficient of Cu-graphite composites, Wear 265 (2008) 417–421. https://doi.org/10.1016/j.wear.2007.11.012
[13] S. B. Cantürk, J. Kováčik, A. Opálek, N. Beronská, Ľ. Orovčík, Changes in the interface microstructure of copper-based composite materials with a carbon prepared by gas pressure, FEMS EUROMAT 23: Book of Abstracts. Germany, 2023, p. 886.
[14] J. Kováčik, Š. Emmer, J. Bielek, Thermal conductivity of Cu-graphite composites, Int. J. Therm. Sci. 90 (2015) 298–302. https://doi.org/10.1016/j.ijthermalsci.2014.12.017
[15] A. S. Kurlov, A. I. Gusev, E. Yu. Gerasimov, I. A. Bobrikov, A. M. Balagurov, A. A. Rempel, Nanocrystalline ordered vanadium carbide: Superlattice and nanostructure, Superlattices and Microstructures 90 (2016) 148–164. https://doi.org/10.1016/j.spmi.2015.12.006 \
[16] R. W. Powers, M. V. Doyle, The diffusion of carbon and oxygen in vanadium, Acta Metall. 6 (1958) 643–646. https://doi.org/10.1016/0001-6160(58)90158-5
[17] R. B. Bird, W. E. Stewart, E. N. Lightfoot, Transport Phenomena, John Wiley & Sons, New York, 1976.
[18] H. Okamoto, C-V (Carbon-Vanadium), J. Phase Equilib. Diffus. 31 (2010) 91–92. https://doi.org/10.1007/s11669-009-9637-4
[19] X. Chong, Y. Jiang, R. Zhou, J. Feng, The effects of ordered carbon vacancies on stability and thermomechanical properties of V_8C_7 compared with VC, Sci. Rep. 6 (2016) 34007. https://doi.org/10.1038/srep34007
[20] X. Chong, Y. Jiang, R. Zhou, J. Feng, Electronic structures mechanical and thermal properties of V–C binary compounds, RSC Adv. 4 (2014) 44959–44971. https://doi.org/10.1039/c4ra07543a
[21] B. Wang, Y. Liu, J. Ye, Mechanical properties and electronic structures of VC, V_4C_3 and V_8C_7 from first principles, Phys. Scr. 88 (2013) 015301. https://doi.org/10.1088/0031-8949/88/01/015301
[22] P. Amaral, J. Fernandes, L. Rosa, D. Martínez, J. Rodríguez, N. Shohoji, Carbide formation of Va-group metals (V, Nb and Ta) in a solar furnace, Int. J. Refract. Met. Hard Mater. 18 (2000) 47–53. https://doi.org/10.1016/s0263-4368(00)00014-7

[23] Y. Hou, S. Otani, T. Tanaka, Y. Ishizawa, Preparation of vanadium carbide single crystals by a floating zone technique, J. Cryst. Growth 68 (1984) 733–740. https://doi.org/10.1016/0022-0248(84)90112-x

[24] M. Turchanin, P. Agraval, A. Abdulov, Phase equilibria and thermodynamics of binary copper systems with 3*d*-metals. IV. Copper-manganese system, Powder Metall. Met. Ceram. 45 (2006) 569–581. https://doi.org/10.1007/s11106-006-0121-y

[25] R. W. G. Wyckoff, Crystal Structures. Interscience Publishers, New York, 1963, pp. 385–237.

[26] P. Scott, M. Nicholas, B. Dewar, The wetting and bonding of diamonds by copper-base binary alloys, J. Mater. Sci. 10 (1975) 1833–1840. https://doi.org/10.1007/bf00754470

[27] Y. Ding, J. Gao, Y. Han, M. Zhou, H. Wang, C. Zhang, J. Liu, Y. C. Wang, Z. Ding, J. Wang, Z. X. Zhu, Study on the microstructure and properties of copper/graphite composites with two-step method and copper-modified graphite, J. Phys.: Conf. Ser. 2639 (2023) 012021. https://doi.org/10.1088/1742-6596/2639/1/012021

[28] Y. Su, F. Jiang, Z. Xiao, F. Wu, M. Long, Microstructure and tribological properties of copper/graphite composites with Ti_3AlC_2 addition prepared by rapid hot press sintering, Tribol. Int. 194 (2024)109537. https://doi.org/10.1016/j.triboint.2024.109537

[29] X. Jiang, H. C. Fang, P. Xiao, T. Liu, J. M. Zhu, Y. C. Wang, P. F. Liu, Y. Li, Influence of carbon coating with phenolic resin in natural graphite on the microstructures and properties of graphite/copper composites, J. Alloys Compd. 744 (2018) 165–173. https://doi.org/10.1016/j.jallcom.2018.02.051

[30] B. Wang, Y. Liu, J. Ye, Mechanical properties and electronic structures of VC, V_4C_3 and V_8C_7 from first principles, Phys. Scr. 88 (2013) 015301. https://doi.org/10.1088/0031-8949/88/01/015301

[31] J. Kováčik, Š. Emmer, J. Bielek, Cross-property connections for copper-graphite composites, Acta Mech. 227 (2016) 105–112. https://doi.org/10.1007/s00707-015-1411-6

[32] Q. Cui, C. Chen, C. Yu, T. Lu, H. Long, S. Yan, J. Hao, Effect of molybdenum particles on thermal and mechanical properties of graphite flake/copper composites, Carbon 161 (2020) 169–180. http://dx.doi.org/10.1016/j.carbon.2020.01.059

[33] H. Bai, C. Xue, J. L. Lyu, J. Li, G. X. Chen, J. H. Yu, L. M. Xiong, Thermal conductivity and mechanical properties of flake graphite/copper composite with a boron carbide-boron nano-layer on graphite surface, Composites Part A: Appl. Sci. Manuf. 106 (2018) 42–51. http://dx.doi.org/10.1016/j.compositesa.2017.11.019

[34] S. Ren, J. Chen, X. He, X. Qu, Effect of matrix-alloying-element chromium on the microstructure and properties of graphite flakes/copper composites fabricated by hot pressing sintering, Carbon 127 (2017) 412–423. http://doi.org/10.1016/j.carbon.2017.11.033

[35] Q. Liu, X. B. He, S. B. Ren, C. Zhang, L. Ting-Ting, X. H. Qu, Thermophysical properties and microstructure of graphite flake/copper composites processed by electroless copper coating, J. Alloys Compd. 587 (2014) 255–259. https://doi.org/10.1016/j.jallcom.2013.09.207

[36] W. Yang, L. Zhou, K. Peng, J. Zhu, L. Wan, Effect of tungsten addition on thermal conductivity of graphite/copper composites, Composites Part B: Eng. 55 (2013) 1–4. https://doi.org/10.1016/j.compositesb.2013.05.023

[37] B. Liu, D. Q. Zhang, X. F. Li, X. H. Guo, J. Shi, Z. J. Liu, Q. G. Guo, The microstructures and properties of graphite flake/copper composites with high volume fractions of graphite flake, New Carbon Mater. 35 (2020) 58–65. https://doi.org/10.1016/S1872-5805(20)60475-9

[38] B. Liu, D. Zhang, X. Li, Z. He, X. Guo, Z. Liu, Q. Guo, Effect of graphite flakes particle sizes on the microstructure and properties of graphite flakes/copper composites, J. Alloys Compd. 766 (2018) 382–390. https://doi.org/10.1016/j.jallcom.2018.06.129

[39] T. Ueno, T. Yoshioka, J. I. Ogawa, N. Ozoe, K. Sato, K. Yoshino, Highly thermal conductive metal/carbon composites by pulsed electric current sintering, Synth. Met. 159 (2009) 2170–2172. https://doi.org/10.1016/j.synthmet.2009.10.006

[40] R. Prieto, J. M. Molina, J. Narciso, E. Louis, Thermal conductivity of graphite flakes-SiC particles/metal composites, Composites Part A: Appl. Sci. Manuf. 42 (2011) 1970–1977. https://doi.org/10.1016/j.compositesa.2011.08.022

[41] K. Jagannadham, Thermal conductivity of copper-graphene composite films synthesized by electrochemical deposition with exfoliated graphene platelets, Metall. Mater. Trans. B 43 (2012) 316–324. https://doi.org/10.1007/s11663-011-9597-z

[42] W. Li, E. A. Olevsky, O. L. Khasanov, C. A. Back, O. Izhvanov, J. Opperman, H. E. Khalifa, Spark plasma sintering of agglomerated vanadium carbide powder, Ceram. Int. 41 (2015) 3748–3759. https://doi.org/10.1016/j.ceramint.2014.11.050

[43] Y. Lin, X. Chong, M. Gan, W. Yu, Z. Li, J. Feng, X. Liang, Y. Jiang, Probing the effect of ordered carbon vacancy on the thermophysical properties of VC_{1-x}: A comprehensive first-principles calculations, Ceram. Int. 49 (2023) 22518–22528. https://doi.org/10.1016/j.ceramint.2023.04.086

[44] J. H. Jang, H. K. Park, J. H. Lee, J. W. Lim, I. H. Oh, Effect of volume fraction and unidirectional orientation controlled graphite on thermal properties of graphite/copper composites, Composites Part B: Eng. 183 (2020) 107735. https://doi.org/10.1016/j.compositesb.2019.107735

[45] R. Zhang, X. He, H. Chen, X. Qu, Effect of alloying element Zr on the microstructure and properties of graphite flake/Cu composites fabricated by vacuum hot pressing, J. Alloys Compd. 770 (2019) 267–275. https://doi.org/10.1016/j.jallcom.2018.08.107

[46] H. Cao, Z. Tan, G. Fan, Q. Guo, Y. Su, Z. Li, D. B. Xiong, Wide and fine alignment control and interface modification for high-performance thermally conductive graphite/copper composite, Composites Part B: Eng. 191 (2020) 107965. https://doi.org/10.1016/j.compositesb.2020.107965

[47] A. Mazloum, J. Kováčik, Š. Emmer, I. Sevostianov, Copper-graphite composites: Cross-property connections between electrical conductivity and thermal expansion coefficient for 0–90 vol.% of graphite, Mathematics and Mechanics of Solids 29 (2024) 2426–2440. https://doi.org/10.1177/10812865221117764

[48] X. Chong, Y. Jiang, R. Zhou, J. Feng, The effects of ordered carbon vacancies on stability and thermomechanical properties of V_8C_7 compared with VC, Sci. Rep. 6 (2016) 34007.
https://doi.org/10.1038/srep34007